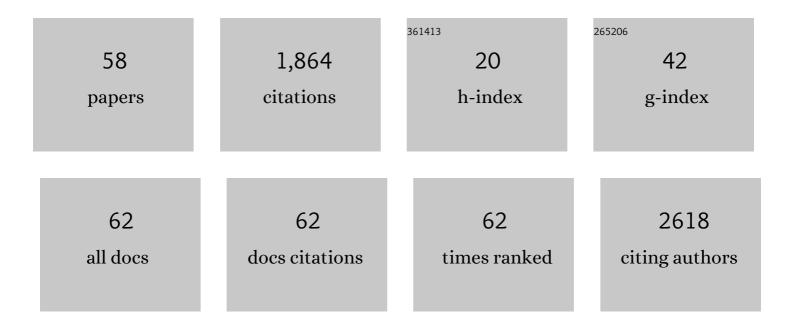
Taylor J Woehl

List of Publications by Year in descending order

Source: https://exaly.com/author-pdf/4311358/publications.pdf Version: 2024-02-01



ΤλΥΙΟΡΙΜΟΕΗΙ

#	Article	IF	CITATIONS
1	Direct <i>in Situ</i> Determination of the Mechanisms Controlling Nanoparticle Nucleation and Growth. ACS Nano, 2012, 6, 8599-8610.	14.6	378
2	Experimental procedures to mitigate electron beam induced artifacts during in situ fluid imaging of nanomaterials. Ultramicroscopy, 2013, 127, 53-63.	1.9	176
3	Direct Observation of Aggregative Nanoparticle Growth: Kinetic Modeling of the Size Distribution and Growth Rate. Nano Letters, 2014, 14, 373-378.	9.1	172
4	Multi-Component Fe–Ni Hydroxide Nanocatalyst for Oxygen Evolution and Methanol Oxidation Reactions under Alkaline Conditions. ACS Catalysis, 2017, 7, 365-379.	11.2	154
5	Direct <i>in Situ</i> Observation of Nanoparticle Synthesis in a Liquid Crystal Surfactant Template. ACS Nano, 2012, 6, 3589-3596.	14.6	93
6	Nucleation of Iron Oxide Nanoparticles Mediated by Mms6 Protein <i>in Situ</i> . ACS Nano, 2014, 8, 9097-9106.	14.6	90
7	The Mechanisms for Nanoparticle Surface Diffusion and Chain Self-Assembly Determined from Real-Time Nanoscale Kinetics in Liquid. Journal of Physical Chemistry C, 2015, 119, 21261-21269.	3.1	86
8	Correlative Electron and Fluorescence Microscopy of Magnetotactic Bacteria in Liquid: Toward In Vivo Imaging. Scientific Reports, 2014, 4, 6854.	3.3	65
9	Quantifying the Nucleation and Growth Kinetics of Electron Beam Nanochemistry with Liquid Cell Scanning Transmission Electron Microscopy. Chemistry of Materials, 2018, 30, 7727-7736.	6.7	61
10	Metal Ionâ€Induced Assembly of MXene Aerogels via Biomimetic Microtextures for Electromagnetic Interference Shielding, Capacitive Deionization, and Microsupercapacitors. Advanced Energy Materials, 2021, 11, 2101494.	19.5	61
11	Minimum Cost Multi-Way Data Association for Optimizing Multitarget Tracking of Interacting Objects. IEEE Transactions on Pattern Analysis and Machine Intelligence, 2015, 37, 611-624.	13.9	60
12	Peptide-Directed PdAu Nanoscale Surface Segregation: Toward Controlled Bimetallic Architecture for Catalytic Materials. ACS Nano, 2016, 10, 8645-8659.	14.6	58
13	Understanding the Role of Solvation Forces on the Preferential Attachment of Nanoparticles in Liquid. ACS Nano, 2016, 10, 181-187.	14.6	51
14	Electron-beam-driven chemical processes during liquid phase transmission electron microscopy. MRS Bulletin, 2020, 45, 746-753.	3.5	38
15	Electrolyte-Dependent Aggregation of Colloidal Particles near Electrodes in Oscillatory Electric Fields. Langmuir, 2014, 30, 4887-4894.	3.5	34
16	Nature of peptide wrapping onto metal nanoparticle catalysts and driving forces for size control. Nanoscale, 2017, 9, 8401-8409.	5.6	29
17	Nanoscale Mapping of Nonuniform Heterogeneous Nucleation Kinetics Mediated by Surface Chemistry. Journal of the American Chemical Society, 2019, 141, 13516-13524.	13.7	29
18	Visualizing Ligand-Mediated Bimetallic Nanocrystal Formation Pathways with <i>in Situ</i> Liquid-Phase Transmission Electron Microscopy Synthesis. ACS Nano, 2021, 15, 2578-2588.	14.6	25

TAYLOR J WOEHL

#	Article	IF	CITATIONS
19	Effects of substrate porosity in carbon aerogel supported copper for electrocatalytic carbon dioxide reduction. Electrochimica Acta, 2019, 297, 545-552.	5.2	24
20	Metal Nanocrystal Formation during Liquid Phase Transmission Electron Microscopy: Thermodynamics and Kinetics of Precursor Conversion, Nucleation, and Growth. Chemistry of Materials, 2020, 32, 7569-7581.	6.7	22
21	Dark-Field Scanning Transmission Ion Microscopy via Detection of Forward-Scattered Helium Ions with a Microchannel Plate. Microscopy and Microanalysis, 2016, 22, 544-550.	0.4	16
22	Quantification of rhenium oxide dispersion on zeolite: Effect of zeolite acidity and mesoporosity. Journal of Catalysis, 2019, 372, 128-141.	6.2	16
23	Visualization of Iron-Binding Micelles in Acidic Recombinant Biomineralization Protein, MamC. Journal of Nanomaterials, 2014, 2014, 1-7.	2.7	15
24	Revealing Reactions between the Electron Beam and Nanoparticle Capping Ligands with Correlative Fluorescence and Liquid-Phase Electron Microscopy. ACS Applied Materials & Interfaces, 2021, 13, 37553-37562.	8.0	15
25	Mesopore differences between pillared lamellar MFI and MWW zeolites probed by atomic layer deposition of titania and consequences on photocatalysis. Microporous and Mesoporous Materials, 2019, 276, 260-269.	4.4	11
26	Toward a modular multi-material nanoparticle synthesis and assembly strategy via bionanocombinatorics: bifunctional peptides for linking Au and Ag nanomaterials. Physical Chemistry Chemical Physics, 2016, 18, 30845-30856.	2.8	10
27	Refocusing <i>in Situ</i> Electron Microscopy: Moving beyond Visualization of Nanoparticle Self-Assembly To Gain Practical Insights into Advanced Material Fabrication. ACS Nano, 2019, 13, 12272-12279.	14.6	10
28	Effects of Protein Unfolding on Aggregation and Gelation in Lysozyme Solutions. Biomolecules, 2020, 10, 1262.	4.0	10
29	Dark-field image contrast in transmission scanning electron microscopy: Effects of substrate thickness and detector collection angle. Ultramicroscopy, 2016, 171, 166-176.	1.9	8
30	Irreversible Nature of Mesoscopic Aggregates in Lysozyme Solutions. Colloid Journal, 2019, 81, 546-554.	1.3	8
31	pH-Mediated Aggregation-to-Separation Transition for Colloids Near Electrodes in Oscillatory Electric Fields. Langmuir, 2021, 37, 9346-9355.	3.5	7
32	Structurally colored protease responsive nanoparticle hydrogels with degradation-directed assembly. Nanoscale, 2019, 11, 17904-17912.	5.6	6
33	Direct Visualization of Planar Assembly of Plasmonic Nanoparticles Adjacent to Electrodes in Oscillatory Electric Fields. Langmuir, 2018, 34, 6237-6248.	3.5	5
34	Directional Statistics of Preferential Orientations of Two Shapes in Their Aggregate and Its Application to Nanoparticle Aggregation. Technometrics, 2018, 60, 332-344.	1.9	5
35	Detection and Sizing of Submicron Particles in Biologics With Interferometric Scattering Microscopy. Journal of Pharmaceutical Sciences, 2020, 109, 881-890.	3.3	4
36	Harnessing Control of Radiolysis during Liquid Cell Electron Microscopy to Enable Visualization of Nanomaterial Transformation Dynamics. Microscopy and Microanalysis, 2016, 22, 40-41.	0.4	3

TAYLOR J WOEHL

#	Article	IF	CITATIONS
37	Toward Quantitative Liquid Cell Electron Microscopy through Kinetic Control of Solution Chemistry. Microscopy and Microanalysis, 2019, 25, 23-24.	0.4	2
38	Real-time imaging of metallic supraparticle assembly during nanoparticle synthesis. Nanoscale, 2022, 14, 312-319.	5.6	2
39	Correlative Fluorescence and Liquid Cell STEM of Live Magnetotactic Bacteria. Microscopy and Microanalysis, 2014, 20, 1510-1511.	0.4	1
40	Implementing in situ Experiments in Liquids in the (Scanning) Transmission Electron Microscope ((S)TEM) and Dynamic TEM (DTEM). Microscopy and Microanalysis, 2014, 20, 1648-1649.	0.4	1
41	Correlative Electron and Fluorescence Microscopy of Magnetotactic Bacteria in Liquid: Toward In Vivo Imaging. Microscopy and Microanalysis, 2015, 21, 1499-1500.	0.4	1
42	The Mechanisms for Preferential Attachment of Nanoparticles in Liquid Determined Using Liquid Cell Electron Microscopy, Machine Learning, and Molecular Dynamics. Microscopy and Microanalysis, 2016, 22, 812-813.	0.4	1
43	A Fluorescence Microscopy Assay for Assessing Beam Damage to Nanoparticle Capping Ligands During Liquid Cell Electron Microscopy. Microscopy and Microanalysis, 2019, 25, 1672-1673.	0.4	1
44	Protein-Mediated Nucleation of Nanoparticles In-Situ. Microscopy and Microanalysis, 2014, 20, 1604-1605.	0.4	0
45	Direct Observation of Aggregative Nanoparticle Growth: Kinetic Modeling of the Size Distribution and Growth Rate. Microscopy and Microanalysis, 2014, 20, 1612-1613.	0.4	0
46	An Analytical Scattering Model for Low Energy Annular Dark Field Transmission Scanning Electron Microscopy. Microscopy and Microanalysis, 2015, 21, 1263-1264.	0.4	0
47	Visualization of Gold Nanoparticle Self-assembly Kinetics. Microscopy and Microanalysis, 2015, 21, 945-946.	0.4	0
48	Correlative in situ Analysis of Magnetosome Magnetite Biomineralization. Microscopy and Microanalysis, 2016, 22, 12-13.	0.4	0
49	Control of Radiation Chemistry during Liquid Cell TEM to Synthesize Transition Metal and Bimetallic Nanoparticles. Microscopy and Microanalysis, 2017, 23, 854-855.	0.4	0
50	Utilizing Electron Beam Control and Radiation Chemistry during Liquid Cell Electron Microscopy to Image Protein Aggregates in their Native Hydrated State. Microscopy and Microanalysis, 2018, 24, 1976-1977.	0.4	0
51	Quantitative Modeling of Kinetically Controlled Nanocrystal Synthesis with Liquid Cell Electron Microscopy. Microscopy and Microanalysis, 2018, 24, 280-281.	0.4	0
52	Visualizing Platinum Supraparticle Formation with Liquid Cell Electron Microscopy and Correlative Investigation of Catalytic Activity. Microscopy and Microanalysis, 2019, 25, 2026-2027.	0.4	0
53	Probing the Surface Structure of Monoclonal Antibody Aggregates with Multiscale Microscopy. Microscopy and Microanalysis, 2020, 26, 1068-1069.	0.4	0
54	Establishing Flask-Relevant Reaction Conditions for Imaging Bimetallic Nanocrystal Formation with Liquid Phase Transmission Electron Microscopy. Microscopy and Microanalysis, 2020, 26, 2568-2570.	0.4	0

TAYLOR J WOEHL

#	Article	IF	CITATIONS
55	Visualizing non-classical formation pathways of alloyed nanocrystals with liquid phase transmission electron microscopy. Microscopy and Microanalysis, 2021, 27, 2634-2635.	0.4	Ο
56	Investigating electron beam interactions with nanoparticle capping ligands using correlative liquid phase transmission electron microscopy and fluorescence microscopy. Microscopy and Microanalysis, 2021, 27, 2624-2625.	0.4	0
57	Probing Electron Beam – Nanoparticle Capping Ligand Interactions during Liquid Phase Transmission Electron Microscopy Using a Correlative Fluorescence Microscopy Assay. Microscopy and Microanalysis, 2021, 27, 21-22.	0.4	Ο
58	Chemically fueled assembly of protein hydrogels driven by a redox cycle. Biophysical Journal, 2022, 121, 151a.	0.5	0